Ink4a and Arf are crucial factors in the determination of the cell of origin and the therapeutic sensitivity of Myc-induced mouse lymphoid tumor

Eiji Sugihara[1,2], **Takatsune Shimizu**[1,2], **Kensuke Kojima**[3], **Nobuyuki Onishi**[1], **Kazuharu Kai**[1], **Jo Ishizawa**[1], **Keiko Nagata**[4], **Norisato Hashimoto**[1], **Hiroaki Honda**[5], **Masamoto Kanno**[6], **Masanao Miwa**[7], **Seiji Okada**[8], **Michael Andreeff**[3], and **Hideyuki Saya**[1,2]

[1]Division of Gene Regulation, Institute for Advanced Medical Research, School of Medicine, Keio University, Tokyo, Japan

[2]Japan Science and Technology Agency, CREST, Tokyo, Japan

[3]Section of Molecular Hematology and Therapy, Department of Leukemia, M.D. Anderson Cancer Center, University of Texas, Houston

[4]Drug Discovery Research Laboratories, Kyowa Hakko Kirin Co., Ltd., Shizuoka, Japan

[5]Department of Disease Model, Research Institute of Radiation Biology and Medicine, Hiroshima University, Hiroshima, Japan

[6]Department of Immunology, Graduate School of Biosciences, Hiroshima University, Hiroshima, Japan

[7]Nagahama Institute of Bio-Science and Technology, Shiga, Japan

[8]Division of Hematopoiesis, Center for AIDS Research, Kumamoto University, Kumamoto, Japan

Abstract

The cell of origin of tumors and the the factors determining the cell of origin remain unclear. In this study, a mouse model of precursor-B acute lymphoblastic leukemia/lymphoma (pre-B ALL/LBL) was established by retroviral transduction of *Myc* genes (*N-Myc* or *c-Myc*) into mouse bone marrow cells. Hematopoietic stem cells (HSCs) exhibited the highest susceptibility to N-Myc-induced pre-B ALL/LBL versus lymphoid progenitors, myeloid progenitors and committed progenitor B cells. N-Myc was able to induce pre-B ALL/LBL directly from progenitor B cells in the absence of *Ink4a* and *Arf*. *Arf* was expressed higher in progenitor B cells than *Ink4a*. In addition, N-Myc induced pre-B ALL/LBL from *Arf*$^{-/-}$ progenitor B cells, suggesting that Arf plays a predominant role in determining the cell of origin of pre-B ALL/LBL. Tumor cells derived from *Ink4a/Arf*$^{-/-}$ progenitor B cells exhibited a higher rate of proliferation and were more

chemoresistant than those derived from wild-type HSCs. Furthermore, the Mdm2 inhibitor Nutlin-3 restored p53 and induced massive apoptosis in mouse pre-B ALL/LBL cells derived from *Ink4a/Arf$^{-/-}$* cells and human B-ALL cell lines lacking *Ink4a* and *Arf* expression, suggesting that Mdm2 inhibition may be a novel therapeutic approach to the treatment of *Ink4a/Arf$^{-/-}$* B-ALL/LBL, such as is frequently found in Ph$^+$ ALL and relapsed ALL. Collectively, these findings indicate that Ink4a and Arf are critical determining factors of the cell of origin and the therapeutic sensitivity of Myc-induced lymphoid tumors.

Keywords

Myc; cell of origin; Ink4a; Arf; pre-B ALL/LBL; Mdm2 inhibitor

Introduction

Understanding the cell of origin of tumors is important not only for elucidating detailed mechanisms of tumorigenesis but also for characterizing the context in which tumor cells develop, both of which provide useful information that can inform preventive therapy and therapeutic strategies in the clinical setting (Visvader 2011). Stem cells and multi-potent progenitor cells are believed to be prone to tumors because their cellular characteristics are similar to tumor cells. We recently demonstrated that well-differentiated osteosarcomas arise from immature bone marrow stromal cells, including mesenchymal stem cells, as the cell of origin, in a mouse model (Shimizu et al 2010). However, it remains unresolved whether the cell of origin of hematopoietic malignancies, such as B cell lymphoid tumors composed of differentiated tumor cells, is derived from stem cells, progenitor cells or committed (differentiated) cells (Cobaleda and Sanchez-Garcia 2009). Furthermore, to date, only a few studies have compared the characteristics of tumor cells derived from distinct cells of origin.

Deregulated expression of *Myc* oncogenes (*c-Myc*, *N-Myc* and *L-Myc*) is frequently found in solid tumors as well as hematopoietic tumors, and is often associated with a poor prognosis (Meyer and Penn 2008). Myc is a potent oncogene that can directly induce hematopoietic tumors such as Burkitt's lymphoma, acute myeloid leukemia and acute lymphoid leukemia (ALL) in mouse models (Adams et al 1985, Luo et al 2005, Kawagoe et al 2007). In Eμ-*Myc* transgenic mice, animals develop lymphoid tumors that are likely derived from committed B cells, since *Myc* expression in this model is controlled by the immunogloblin enhancer-promoter (Adams et al 1985). On the other hand, enhanced expression of *c-Myc* in fetal liver cells, including mainly hematopoietic stem and progenitor cells, induces committed B cell lymphoma (Hemann et al 2005). Thus, stem cells, progenitor cells and differentiated cells could be the cell of origin for lymphoid tumors induced by Myc.

To clarify the cell of origin of hematopoietic tumors, we introduced the *Myc* oncogene into various fractions of mouse bone marrow mononuclear cells (BM-MNCs). Both HSCs and committed progenitor B cells were able to serve as the cell of origin for precursor B acute lymphoblastic leukemia/lymphoma (pre-B ALL/LBL) induced by Myc, but the development of pre-B ALL/LBL directly from progenitor B cells was subject to certain molecular limitations. Furthermore, the therapeutic outcomes were different depending on the cell of

origin, even though the tumor cells were similar in terms of immunophenotype and histopathology. Our findings implicate a novel therapeutic concept for the treatment of pre-B ALL/LBL derived from distinct cells of origin.

Results

Myc rapidly induces pre-B ALL/LBLin immature BM-MNCs

We attempted to establish the mouse hematopoietic tumor model using BM-MNCs from the adult mouse. We used a conventional method based on the BM transplantation assay because it is easier to establish tumors with short-term latency and to distinguish cell subpopulations by differentiation markers. Given that *N-Myc* recently has been reported to have more tumorigenic activity than *c-Myc* in hematopoietic tumor (Kawagoe et al 2007), we first used *N-Myc* for tumor induction. Retroviral vectors for *N-Myc* and *N-Myc* lacking the *Myc Box II* (MBII) domain, an important region for transactivation, were constructed (Supplementary Figure 1a). BM-MNCs were isolated from mice after 5-FU treatment, which enriches immature cells, and then infected with retroviral vectors. Infected cells were injected intravenously into lethally irradiated mice (Supplementary Figure 1b). Six weeks after transplantation, GFP-positive cells and the number of peripheral blood mononuclear cells (PBMCs) in mice transplanted with *N-Myc*-transduced BM-MNCs were significantly higher than mice transplanted with control- or MBII-transduced cells (Figure 1a and d). All mice transplanted with *N-Myc*-transduced BM-MNCs died after approximately 2 months (Figure 1b). On the other hand, mice transplanted with control- or MBII-transduced cells showed no signs of tumor growth over a period of 300 days. Tumor-bearing mice had enlarged lymph nodes (LNs) and thymus and exhibited splenomegaly (Figure 1c). As seen by H&E staining, tissue destruction was readily apparent in BM, LNs and liver that had been invaded and were occupied by tumor cells (Figure 1d). Flow cytometry analysis showed that almost all tumor cells were negative for the myeloid markers Mac1 and Gr1, positive for the B cell markers B220 and CD19, and positive-to-negative for the precursor B cell marker CD43 (CD43$^+$, pro-B; CD43$^-$, pre-B), and tumor cells were also negative for the mature B cell marker IgM (Figure 1e). Based on histopathology and immunophenotype, the tumors were classified as pre-B ALL/LBL (Morse et al 2002). We further found that transplantation of *c-Myc*-transduced BM-MNCs could also induce lymphoid tumor showing similar latency and immunophenotype to N-Myc-induced pre-B ALL/LBL (Supplementary Figure 1a, c and d). Collectively, these results suggest that both N-Myc and c-Myc commonly induce pre-B ALL/LBL in proliferating immature BM-MNCs.

HSCs exhibits the highest susceptibility to Myc-induced pre-B ALL/LBL, and B220$^+$ tumor cells can serve as the tumor-initiating cells for secondary tumors

HSCs give rise to common lymphoid progenitors (CLPs) and myeloid progenitors (MPs). CLPs are differentiated to committed progenitor B cells that ultimately become mature B cells (Supplementary Figure 2a). To identify the cell of origin of Myc-induced pre-B ALL/LBL, we separated 3 main populations, HSCs, MPs and CLPs in *N-Myc*-transduced BM (GFP$^+$) cells (Figure 2a). MPs (61.9%) constituted the greatest subpopulation in *N-Myc*-transduced BM cells. Sorted cells were transplanted into lethally irradiated mice with supportive BM-MNCs. Based on limiting dilution analysis, as few as 100 HSCs were

sufficient to induce Pre-B ALL/LBL, whereas more than 1,000 CLPs and 10,000 MPs were necessary to induce tumors, and these had longer latencies than HSCs-derived tumors (Table.1). Tumor cells and tissues from mice transplanted with HSCs had a similar immunophenotype (B220$^+$ CD19$^+$ CD43$^{+/-}$ IgM $^-$) and similar histopathology to those derived from *N-Myc*-transduced bulk BM-MNCs (Figure 2b and c). All mice that were injected with CLPs and 2 of the mice transplanted with MPs developed pre-B ALL/LBL (Supplementary Figure 2b and c). The tumor cells of one mouse transplanted with MPs were positive for Gr-1 and slightly positive for CD3 and B220. Although the difference of the frequency in numbers of tumor-initiating cells between HSCs and MPs was statistically significant (*P*<0.01), the difference of the frequency in those cells between HSCs and CLPs was not (*P*=0.261). However, the frequency of tumor initiating cells was 3-fold higher in HSCs (1:184) than in CLPs (1:558). N-Myc did not simply enrich HSCs after retroviral transduction because the populations of *N-Myc*-transduced HSCs, CLPs and MPs were similar to control cells infected with empty vector (Supplementary Figure 2d). Collectively, these results suggest that HSCs are the most likely candidate for the cell of origin of Myc-induced pre-B ALL/LBL in immature BM-MNCs.

We next performed secondary transplantation of pre-B ALL/LBL tumor cells. Interestingly, none of the tumor cells derived from *N-Myc*-transduced HSCs expressed both the HSC markers c-kit and sca-1 (Figure 2d). Therefore, GFP$^+$B220$^+$ BM-MNCs from tumor-bearing mice were sorted and transplanted into sublethally-irradiated mice (Figure 2e). Mice that received a secondary transplant of GFP$^+$B220$^+$ cells developed pre-B ALL/LBL with shorter latency than the primary tumor (Table 2). The frequency of tumor-initiating cells was 1:216 based on limiting dilution analysis. These results suggest that there are tumor-initiating cells capable of developing secondary tumors within the B220$^+$ cell population in the mouse pre-B ALL/LBL model.

Committed progenitor B cells can serve as the cell of origin of Myc-induced pre-B ALL/LBL in the absence of *Ink4a* and *Arf*

To clarify whether committed progenitor B cells can be the cell of origin of N-Myc-induced pre-B ALL/LBL, BM-MNCs were isolated from non-treated mice and then infected with the retroviral expression vector for *N-Myc*. *N-Myc*-transduced progenitor B cells were sorted and transplanted intravenously into irradiated recipients (Figure 3a and b left). Transplanted *N-Myc*-transduced progenitor B cells failed to induce tumors, even when 50,000 cells were injected (Table 3). These data suggest that more highly differentiated cells in the hematopoietic lineage are less susceptible to N-Myc-induced tumorigenesis.

Recent reports have suggested a close correlation between the self-renewing activity of normal tissue stem cells and inactivation of *Ink4a* and *Arf*. We recently showed that loss of *Ink4a* and *Arf* is required for the development of c-Myc-induced osteosarcoma-initiating cells from BM stromal cells (Shimizu et al 2010). Here, we isolated progenitor B cells derived from *Ink4a/Arf* deficient mice (Figure 3b right) and used them for retroviral transduction and transplantation. Mice that received *N-Myc*-transduced *Ink4a/Arf*$^{-/-}$ progenitor B cells developed pre-B ALL/LBL with a shorter latency than mice transplanted with *N-Myc*-transduced WT HSCs (Table 3). As few as 1,000 *Ink4a/Arf*$^{-/-}$ progenitor B

cells were sufficient to induce tumors. Furthermore, tumor cells and tissues exhibited a similar immunophenotype (B220$^+$ CD19$^+$ CD43$^{+/-}$ IgM$^-$) and histopathology to those that originated from WT HSCs (Figure 3c and d). In addition, we found that c-Myc also induced pre-B ALL/LBL from *Ink4a/Arf*$^{-/-}$ progenitor B cells (Supplementary Figure 3a). These results suggest that Myc can directly transform committed progenitor B cells in the absence of *Ink4a* and *Arf*, and that Ink4a and Arf are critical determining factors of the cell of origin.

Tumor cells derived from *Ink4a/Arf*$^{-/-}$ progenitor B cells are more resistant to Ara-C treatment and grew faster than tumor cells derived from WT HSCs

To characterize potential differences in drug sensitivity between pre-B ALL/LBL tumors derived from *N-Myc*-transduced WT HSCs and *Ink4a/Arf*$^{-/-}$ progenitor-B cells, tumor-bearing mice were administered 4 doses of daily intraperitoneal Ara-C (Cano et al 2008), which is a standard chemotherapeutic agent for the treatment of hematopoietic tumors. Four days after the first injection of Ara-C, the number of tumor cells in peripheral blood was decreased in both types of pre-B ALL/LBL mice (Figure 4a). However, tumor cells derived from *Ink4a/Arf*$^{-/-}$ progenitor-B cells had a significantly greater surviving population and exhibited re-growth at a much faster rate than those from WT HSCs (Figure 4a). To confirm this sensitivity to Ara-C *in vitro*, tumor cells were harvested from BM and then cultured for several days before being treated with Ara-C for 48 h. The results of Annexin V staining showed that tumor cells from *Ink4a/Arf*$^{-/-}$ progenitor-B cells had a significantly greater population of surviving cells (Annexin V-negative cells) after Ara-C treatment than those from WT HSCs at several different concentrations of Ara-C (Figure 4b). Moreover, tumor cells from *Ink4a/Arf*$^{-/-}$ progenitor-B cells exhibited a faster growth rate than those from WT HSCs *in vitro* (Figure 4c). These results suggest that tumor cells that lack *Ink4a and Arf* are more refractory to Ara-C treatment and show faster growth.

Arf is a key factor in determining the cell of origin of pre-B ALL/LBL

The expression of *Ink4a* and *Arf* is normally maintained at a low level to endow HSCs with self-renewing capacity. The polycomb protein Bmi1 suppresses the expression of both genes through promoter methylation of the *CDKN2A* locus in HSCs (Park et al 2003, Iwama et al 2004). To analyze how these genes were regulated in committed progenitor B cells, *N-Myc*-transduced HSCs and progenitor B cells from WT mice were fractionated, and the expression of *Ink4a, Arf* and *Bmi1* was measured by quantitative real-time RT-PCR. *Ink4a* expression in *N-Myc*-transduced progenitor B cells was similar to that in HSCs, whereas *Arf* expression was significantly higher (> 200 fold) (Figure 5a). On the other hand, *Bmi1* expression in progenitor B cells was significantly lower than in HSCs. The levels of transduced *N-Myc* expression were similar in both HSCs and progenitor B cells. Moreover, *Arf* expression in progenitor B cells transduced with the control vector was also significantly higher than that in control HSCs (Figure 5b). Thus *N-Myc* transduction did not affect *Arf* expression in HSCs and progenitor B cells, indicating that *Arf* expression is maintained at a high level in progenitor B cells. To clarify whether *Bmi1* overexpression suppresses *Arf* expression in progenitor B cells, the retroviral vector expressing *Bmi1* were infected into progenitor B cells and then mRNA level of *Arf* was measured by quantitative real-time RT-PCR. As a result, *Arf* expression was significantly reduced in *Bmi1*-transduced cells compared with control-transduced cells, suggesting that *Arf* expression in progenitor B cells

depends on *Bmi1* expression (Figure 5c). Collectively, these results raised the possibility that Arf has a key role in blocking N-Myc-induced transformation of progenitor B cells.

To determine a role of Arf in progenitor B cells, $Arf^{-/-}$ progenitor B cells were isolated from *Arf* deficient mice and infected with the retroviral vector expressing *N-Myc*. Transplantation of 10,000 or only 1,000 *N-Myc*-transduced $Arf^{-/-}$ progenitor B cells induced pre-B ALL/LBL with similar immunophenotype (B220$^+$ CD43$^{+/-}$ IgM$^-$) to $Ink4a/Arf^{-/-}$-derived tumor cells (Figure 5d). Thus, these findings suggest that Arf plays a predominant role in determining the cell of origin of pre-B ALL/LBL.

The Mdm2 inhibitor Nutlin-3 restores p53 and thereby effectively induces apoptosis in tumor cells derived from *Ink4a/Arf$^{-/-}$* progenitor B cells

Mdm2, a negative regulator of the tumor suppressor protein p53, functions as an E3 ubiquitin ligase to ubiquitinate p53, which leads to p53 degradation (Wade et al 2010). Nutlin-3 is a small molecule inhibitor that prevents Mdm2 binding to p53 (Vassilev et al 2004) and has recently been evaluated as a novel, targeted agent in leukemia therapy (Kojima et al 2005, Gu et al 2008). Since Arf inhibits Mdm2 binding to p53, we hypothesized that Nutlin-3 might substitute for Arf and reactivate p53 in tumor cells derived from $Ink4a/Arf^{-/-}$ progenitor B cells. Nutlin-3 treatment induced extensive apoptosis in cultured $Ink4a/Arf^{-/-}$ progenitor B cell-derived tumor cells (Figure 6a, left). In fact, all 3 tumor cell clones were effectively killed by Nutlin-3 treatment in a concentration-dependent manner (Figure 6a, right). The sequence of the p53 gene was confirmed as wild-type in all 3 clones. In contrast, Nutlin-3 was relatively ineffective against tumor cells derived from WT HSCs and WT bulk BM cells, which contained mutations in the p53 in the DNA-binding region (Supplementary Figure 4a and b). Following Nutlin-3 treatment, p53 and the apoptosis indicator cleaved caspase-3 were increased in tumor cells derived from $Ink4a/Arf^{-/-}$ cells (Figure 6b). The p53 targets p21 and Mdm2 were also increased by Nutlin-3 treatment. Furthermore, $Ink4a/Arf^{-/-}$-derived tumor cells expressing *p53* shRNA showed significant reduction of Nutlin-3-induced apoptosis compared with those cells expressing control *luciferase* shRNA, confirming that the Nulin-3-induced apoptosis is p53-dependent (Figure 6c).

We next investigated the effect of co-treatment with Ara-C and Nutlin-3 on tumor cells from $Ink4a/Arf^{-/-}$ progenitor B cells. For this analysis, we examined tumor cells of clone 1, as they were less sensitive to 2.5 μM Nutlin-3 compared to the other clones (Figure 6a right). Although treatment with Ara-C (0.25 μg/ml) or Nutlin-3 (2.5 μM) alone did not efficiently induce apoptosis (24.7% and 39.5%, respectively), combination treatment with Ara-C and Nutlin-3 had a synergistic effect on enhancing apoptosis (75.5%) in tumor cells from $Ink4a/Arf^{-/-}$ progenitor B cells (Figure 6d left). Nutlin-3 effectively killed tumor cells when combined with different concentrations of Ara-C (Figure 6d right). Collectively, these data suggest that Nutlin-3 may be effective in eradicating tumor cells lacking *Ink4a* and *Arf*.

Nutlin-3 effectively induces apoptosis in human B-ALL cell lines lacking expression of *Ink4a* and *Arf*

We attempted to apply our finding that lack of *Ink4* and *Arf* expressions and p53 status can affect chemotherapeutic efficacy to human B-ALL cells. Six human B-ALL cell lines including PALL-2, NAGL-1, NALM-6, HAL-01 (these 4 lines have wild-type p53), BALL-1 and Tanoue (both 2 lines have mutated p53: D281G and M246T, respectively) were treated with Nutlin-3 or Ara-C for 48 h. Nutlin-3 treatment significantly induced apoptosis in cell lines with wild-type p53 but not in cell lines with mutated p53 (Figure 7a). Furthermore, real-time quantitative RT-PCR showed that the cell lines with WT p53 did not express *Ink4a* and *Arf* genes whereas the cell lines with mutated p53 express *Ink4a* and/or *Arf* (Figure 7b). In terms of Ara-C sensitivity, p53 status was not a critical determination factor. Because, although BALL-1 cells having mutated p53 were more sensitive to Ara-C treatment than cell lines with wild-type p53, Tanoue cells having mutated p53 were even less sensitive to Ara-C (Supplementary Figure 4c). Collectively, these results suggest that Nutlin-3 effectively induces apoptosis in human B-ALL cell lines with wild-type p53 and lacking expression of *Ink4a* and *Arf*, which is a similar result to mouse pre-B ALL/LBL cells.

Discussion

In this study, we demonstrated that N-Myc rapidly induced pre-B ALL/LBL originated from HSCs, whereas it could not induce any tumor directly from committed progenitor B cells due to limiting factors Ink4a and Arf. Furthermore, tumor cells derived from distinct cells of origin showed different drug sensitivities to Ara-C and Nutlin-3, which provides a novel insight into preventive therapy and different therapeutic approaches depending on genetic background of tumor cells (Figure 7c). In our mouse model, there is no significant difference between two types of *Myc* oncogenes, *N-Myc* and *c-Myc*, in respect to tumorigenic activities and chemotherapeutic sensitivities of the induced tumors (Figure 4b, 6a and Supplementary Figure 3b and c). Overexpression of these *Myc* genes has been reported in a number of B-ALL patients, suggesting a pathophysiological relevance between Myc and human B-ALL (Cardone et al 2005).

Tumor-initiating cells in human B-ALL that have the potential to self-renew and generate secondary tumors reportedly express normal HSC markers, i.e., CD34^{+}, CD38^{−}, and/or B cell markers, i.e., CD10^{+}, CD19^{+} (Cobaleda et al 2000, Cox et al 2004, Castor et al 2005, Hotfilder et al 2005, Hong et al 2008, le Viseur et al 2008). In the current syngenic mouse model, tumor-initiating cells capable of generating secondary tumors were identified in the B cell marker-positive cell population, not the HSC marker-positive cell population, which corroborates the fact that there are tumor-initiating cells that are positive for B cell markers in human B-ALL. Interestingly, the tumor-initiating cells that develop primary tumors were part of the HSC marker-positive cell population. This difference in the tumor initiating cells between primary and secondary tumors indicates that HSCs that express *Myc* can essentially disappear, developing into committed progenitor B cells during transformation. Previous reports have suggested that the enhanced expression of *Myc* results in the migration of HSCs from the BM niche, thereby promoting the commitment to progenitor cells (Wilson et al

2004). The expansion and transformation of *Myc*-transduced cells is believed to occur at the stage of progenitor B cell. Recently, it was reported that c-Myc is involved in the regulation of pro-B expansion as a downstream effector in the MAPK signaling pathway (Yasuda et al 2008), which suggests that progenitor B cells are the most suitable candidate for Myc-induced expansion. Our findings raise the possibility that *Myc*-transduced HSCs initially give rise to multi-hematopoietic lineages, and then progenitor B cells gain a Myc-induced proliferative advantage and become dominant. Ultimately, these expanding progenitor B cells acquire additional mutations, e.g., p53 mutations, and become fully transformed.

The cell of origin of B-ALL has long been debated and is assumed to be stem cell or immature progenitor cell (Cobaleda and Sanchez-Garcia 2009). We demonstrated that HSCs from the BM of adult mice are the primary origin/target in pre-B ALL/LBL. HSCs express functional Bmi1, which suppresses the expression of *Ink4a* and *Arf* and enables the cells to maintain their self-renewing capacity. Bmi1 has been reported to suppress Arf-dependent apoptosis induced by Myc to enhance lymphomagenesis (Jacobs et al 1999). It is possible that HSCs are more potent to receive *N-Myc* overexpression without inducing apoptosis. On the other hand, no tumors were induced directly from WT committed progenitor B cells. Given that *Arf* is expressed in progenitor B cells much higher than *Ink4a*, and that N-Myc was able to induce tumor derived from $Arf^{-/-}$ progenitor B cells, Arf represents a predominant factor in the determination of the cell of origin of Myc-induced pre-B ALL/LBL, similar to its role in the mouse model of BCR-ABL-induced B-ALL (Wang et al 2008). It should be noted that tumor cells derived from WT cells carried mutations in p53, indicating that inactivation of the Arf-p53 pathway is critical for B lymphoid tumorigenesis, consistent with previous results (Eischen et al 1999).

Following Ara-C treatment *in vitro* and *in vivo*, tumor cells derived from $Ink4a/Arf^{-/-}$ progenitor B cells were more refractory to apoptosis and showed faster re-growth compared to those derived from WT HSCs. Previous reports suggest that $Ink4a/Arf^{-/-}$ lymphoma cells display reduced p53 activity and thereby escape from apoptosis and/or senescence programs induced by p53 and Ink4a (Schmitt et al 1999, Schmitt et al 2002). Fast growth of $Ink4a/Arf^{-/-}$ tumor cells may arise from a fact that *Arf*-null pre-B cells show canceling Arf-p53 checkpoint and thus promote Myc-induced proliferation (Eischen et al 1999). Although tumors that originated from WT HSCs carried mutated p53, these cells expressed high levels of *Ink4a* and *Arf* (Supplementary Figure 4d). Ink4a and Arf play crucial roles in the induction of apoptosis and Arf can also induce apoptosis independently of p53 (Ausserlechner et al 2001, Tsuji et al 2002). The heightened sensitivity of tumor cells from WT HSCs to Ara-C treatment compared to those from $Ink4a/Arf^{-/-}$ progenitor B cells may reflect a p53-independent mechanism of apoptosis by Ink4a and Arf.

The *CDKN2A* locus is deleted or inactivated in nearly half of all cases of B-ALL, especially Ph[+] B-ALL and recurrent types of B-ALL (Mullighan et al 2008a, Mullighan et al 2008b). To date, there has not been a good mouse model for understanding and developing treatments for these types of malignant ALL. The mouse model of pre-B ALL/LBL derived from $Ink4a/Arf^{-/-}$ progenitor B cells developed in the current study could be such a suitable model. In testing novel therapeutic approaches with this model, we used Nutlin-3 to inhibit p53-Mdm2 binding because all of the tumor clones derived from $Ink4a/Arf^{-/-}$ progenitor B

cells had wild-type p53, and *p53* gene mutations are relatively infrequent in cases of CML-lymphoid blast crisis, in which *Arf* loss predominates (Calabretta and Perrotti 2004). We demonstrated that Nutlin-3 treatment reactivated p53 and drastically induced apoptosis in tumor cells derived from *Ink4a/Arf*$^{-/-}$ progenitor B cells. Recently, it was reported that Nutlin-3 is effective against human B-ALL cells with wild-type p53 (Gu et al 2008). We found that Nutlin-3 treatment effectively induced apoptosis in human B-ALL cell lines with wild-type p53 and lacking *Ink4a* and *Arf* expression, and thereby the concept we obtained from our established pre-B ALL/LBL mouse model can be applied to human B-ALL. We further tested combination treatment with Ara-C and Nutlin-3 in consideration of the clinical setting (Kojima et al 2006). In this case, relatively low dose of Nutlin-3 acted synergistically to enhance apoptosis induced by Ara-C in tumor cells derived from *Ink4a/Arf*$^{-/-}$ progenitor B cells. These results suggest that the upregulation of p53 by Nutlin-3 enhances Ara-C-induced apoptosis. If a tumor is classified as pre B-ALL according to histopathology and immunophenotype, additional analysis to determine genetic background, such as *p53* mutation or *Ink4a/Arf* inactivation, could inform the most appropriate therapeutic strategy for an individual patient.

Materials and Methods

Mice

Wild-type C57BL/6 mice (6- to 8-weeks-old) were purchased from Charles River Japan Inc. (Atsugi, Japan). *Ink4a/Arf*$^{-/-}$ mice (B6.129-*Cdkn2a*^{tm1Rdp}) were obtained from Mouse Models of Human Cancers Consortium (NCI-Frederick). *Arf*$^{-/-}$ mice were described previously (Kamijo et al 1997) and kindly provided by C.J. Sherr (St. Jude Children's Hospital). Animals were cared for in accordance with the guidelines of the Keio University School of Medicine.

Human cell lines

Two human B-ALL cell lines PALL-2 and NAGL-1 were obtained from HSRRB (Osaka, Japan). The other human B-ALL cell lines NALM-6, HAL-01, BALL-1 and Tanoue were obtained from RIKEN Cell Bank (Tsukuba Japan). NAGL-1 was maintained in IMDM (Invitrogen, San Diego, CA) supplemented with 20% FCS and the other cell lines were maintained in RPMI (Sigma, St. Louis, MO) supplemented with 10% FCS at 37 °C in 5% CO_2 and 100% humidity.

Retroviral vectors, transduction and bone marrow transplant assay

Mouse *N-Myc* and *MBII* cDNAs were cloned into the retroviral vector pMXs-IG. Mouse *Bmi1 cDNA* was cloned into pMXs-IRES-DsRed. The empty vector was used as a control. The pMX-based vectors were transfected into Plat-E packaging cells (Morita et al 2000) using Fugene HD (Roche, Mannheim, Germany) and then the cells were allowed to incubate overnight at 37 °C in 5% CO_2. The medium was replaced 24 h after transfection. Viral supernatants were filtered using a 0.45-μm cellulose acetate filter (Iwaki, Tokyo, Japan) after 48 h of incubation. Procedures of retroviral infection and bone marrow transplant assay are described in Supplementary Methods.

Flow cytometry

BM-MNCs from tumor-bearing mice were stained with allophycocyanin (APC)-conjugated anti-B220, phycoerythrin (PE)-conjugated CD43, CD19 (all from Biolegend, San Diego, CA), and IgM antibodies (eBioscience, San Diego, CA). Samples were analyzed using a FACSCalibur system (BD Biosciences, San Diego, CA). Cell sorting is described in Supplementary Methods.

Ara-C and Nutlin-3 treatment

Tumor-bearing mice were treated intraperitoneally with 100 mg/kg of cytosine arabinoside (Ara-C, Sigma) for 4 consecutive days. Peripheral blood (PB) was lysed with red blood cell lysis buffer and then counted. For the apoptosis assay, cells were incubated in the presence or absence of Ara-C and/or Nutlin-3 (Kojima et al 2005) for 48 h. Assays for detection of apoptosis and BrdU incorporation are described in Supplementary Methods.

Immunoblot analysis

Cells were lysed and denatured as previously described (Sugihara et al 2006). Samples were separated by SDS-PAGE and then proteins were transferred to a PVDF membrane (GE Healthcare, Piscataway, NJ). Membranes were incubated for 1 h at room temperature in blocking buffer consisting of 5% nonfat dry milk in PBS with 0.05% Tween 20, followed by an appropriate dilution of anti-p53 (FL-393), anti-Mdm2 (SMP14), anti-p21 (C-19), (all from Santa Cruz Biotechnology, Santa Cruz, CA), anti-cleaved caspase-3 (Cell Signaling Technology, Danvers, MA) or anti-α-tubulin (Sigma) primary antibody overnight at 4 °C. Membranes were incubated with horseradish peroxidase-conjugated secondary antibody (GE Healthcare) for 45 min at room temperature. Peroxidase activity was detected by Western lightning chemiluminescence reagents (Perkin Elmer, Boston, MA, USA).

Statistical analysis

Differences between two groups were compared using the two-tailed unpaired Student's t-test. P values in frequency of tumor-initiating cells based on limiting dilution analysis were calculated with ELDA (Hu and Smyth 2009). $P < 0.05$ was considered statistically significant.

Supplementary Material

Refer to Web version on PubMed Central for supplementary material.

Acknowledgments

References

Adams JM, Harris AW, Pinkert CA, Corcoran LM, Alexander WS, Cory S, et al. The c-myc oncogene driven by immunoglobulin enhancers induces lymphoid malignancy in transgenic mice. Nature. 1985; 318:533–538. [PubMed: 3906410]

Ausserlechner MJ, Obexer P, Wiegers GJ, Hartmann BL, Geley S, Kofler R. The cell cycle inhibitor p16(INK4A) sensitizes lymphoblastic leukemia cells to apoptosis by physiologic glucocorticoid levels. J Biol Chem. 2001; 276:10984–10989.

Calabretta B, Perrotti D. The biology of CML blast crisis. Blood. 2004; 103:4010–4022. [PubMed: 14982876]

Cano F, Pannel R, Follows GA, Rabbitts TH. Preclinical modeling of cytosine arabinoside response in Mll-Enl translocator mouse leukemias. Mol Cancer Ther. 2008; 7:730–735. [PubMed: 18347158]

Cardone M, Kandilci A, Carella C, Nilsson JA, Brennan JA, Sirma S, et al. The novel ETS factor TEL2 cooperates with Myc in B lymphomagenesis. Mol Cell Biol. 2005; 25:2395–2405. [PubMed: 15743832]

Castor A, Nilsson L, Astrand-Grundstrom I, Buitenhuis M, Ramirez C, Anderson K, et al. Distinct patterns of hematopoietic stem cell involvement in acute lymphoblastic leukemia. Nat Med. 2005; 11:630–637. [PubMed: 15908956]

Cobaleda C, Gutierrez-Cianca N, Perez-Losada J, Flores T, Garcia-Sanz R, Gonzalez M, et al. A primitive hematopoietic cell is the target for the leukemic transformation in human philadelphia-positive acute lymphoblastic leukemia. Blood. 2000; 95:1007–1013. [PubMed: 10648416]

Cobaleda C, Sanchez-Garcia I. B-cell acute lymphoblastic leukaemia: towards understanding its cellular origin. Bioessays. 2009; 31:600–609. [PubMed: 19444834]

Cox CV, Evely RS, Oakhill A, Pamphilon DH, Goulden NJ, Blair A. Characterization of acute lymphoblastic leukemia progenitor cells. Blood. 2004; 104:2919–2925. [PubMed: 15242869]

Eischen CM, Weber JD, Roussel MF, Sherr CJ, Cleveland JL. Disruption of the ARF-Mdm2-p53 tumor suppressor pathway in Myc-induced lymphomagenesis. Genes Dev. 1999; 13:2658–2669. [PubMed: 10541552]

Gu L, Zhu N, Findley HW, Zhou M. MDM2 antagonist nutlin-3 is a potent inducer of apoptosis in pediatric acute lymphoblastic leukemia cells with wild-type p53 and overexpression of MDM2. Leukemia. 2008; 22:730–739. [PubMed: 18273046]

Hemann MT, Bric A, Teruya-Feldstein J, Herbst A, Nilsson JA, Cordon-Cardo C, et al. Evasion of the p53 tumour surveillance network by tumour-derived MYC mutants. Nature. 2005; 436:807–811. [PubMed: 16094360]

Hong D, Gupta R, Ancliff P, Atzberger A, Brown J, Soneji S, et al. Initiating and cancer-propagating cells in TEL-AML1-associated childhood leukemia. Science. 2008; 319:336–339. [PubMed: 18202291]

Hotfilder M, Rottgers S, Rosemann A, Schrauder A, Schrappe M, Pieters R, et al. Leukemic stem cells in childhood high-risk ALL/t(9;22) and t(4;11) are present in primitive lymphoid-restricted CD34+CD19- cells. Cancer Res. 2005; 65:1442–1449. [PubMed: 15735032]

Hu Y, Smyth GK. ELDA: extreme limiting dilution analysis for comparing depleted and enriched populations in stem cell and other assays. J Immunol Methods. 2009; 347:70–78. [PubMed: 19567251]

Iwama A, Oguro H, Negishi M, Kato Y, Morita Y, Tsukui H, et al. Enhanced self-renewal of hematopoietic stem cells mediated by the polycomb gene product Bmi-1. Immunity. 2004; 21:843–851. [PubMed: 15589172]

Jacobs JJ, Scheijen B, Voncken JW, Kieboom K, Berns A, van Lohuizen M. Bmi-1 collaborates with c-Myc in tumorigenesis by inhibiting c-Myc-induced apoptosis via INK4a/ARF. Genes Dev. 1999; 13:2678–2690. [PubMed: 10541554]

Kamijo T, Zindy F, Roussel MF, Quelle DE, Downing JR, Ashmun RA, et al. Tumor suppression at the mouse INK4a locus mediated by the alternative reading frame product p19ARF. Cell. 1997; 91:649–659. [PubMed: 9393858]

Kawagoe H, Kandilci A, Kranenburg TA, Grosveld GC. Overexpression of N-Myc rapidly causes acute myeloid leukemia in mice. Cancer Res. 2007; 67:10677–10685. [PubMed: 18006809]

Kojima K, Konopleva M, Samudio IJ, Shikami M, Cabreira-Hansen M, McQueen T, et al. MDM2 antagonists induce p53-dependent apoptosis in AML: implications for leukemia therapy. Blood. 2005; 106:3150–3159. [PubMed: 16014563]

Kojima K, Konopleva M, McQueen T, O'Brien S, Plunkett W, Andreeff M. Mdm2 inhibitor Nutlin-3a induces p53-mediated apoptosis by transcription-dependent and transcription-independent mechanisms and may overcome Atm-mediated resistance to fludarabine in chronic lymphocytic leukemia. Blood. 2006; 108:993–1000. [PubMed: 16543464]

le Viseur C, Hotfilder M, Bomken S, Wilson K, Rottgers S, Schrauder A, et al. In childhood acute lymphoblastic leukemia, blasts at different stages of immunophenotypic maturation have stem cell properties. Cancer Cell. 2008; 14:47–58. [PubMed: 18598943]

Luo H, Li Q, O'Neal J, Kreisel F, Le Beau MM, Tomasson MH. c-Myc rapidly induces acute myeloid leukemia in mice without evidence of lymphoma-associated antiapoptotic mutations. Blood. 2005; 106:2452–2461. [PubMed: 15972450]

Meyer N, Penn LZ. Reflecting on 25 years with MYC. Nat Rev Cancer. 2008; 8:976–990. [PubMed: 19029958]

Morita S, Kojima T, Kitamura T. Plat-E: an efficient and stable system for transient packaging of retroviruses. Gene Ther. 2000; 7:1063–1066. [PubMed: 10871756]

Morse HC 3rd, Anver MR, Fredrickson TN, Haines DC, Harris AW, Harris NL, et al. Bethesda proposals for classification of lymphoid neoplasms in mice. Blood. 2002; 100:246–258. [PubMed: 12070034]

Mullighan CG, Phillips LA, Su X, Ma J, Miller CB, Shurtleff SA, et al. Genomic analysis of the clonal origins of relapsed acute lymphoblastic leukemia. Science. 2008a; 322:1377–1380. [PubMed: 19039135]

Mullighan CG, Williams RT, Downing JR, Sherr CJ. Failure of CDKN2A/B (INK4A/B-ARF)-mediated tumor suppression and resistance to targeted therapy in acute lymphoblastic leukemia induced by BCR-ABL. Genes Dev. 2008b; 22:1411–1415. [PubMed: 18519632]

Park IK, Qian D, Kiel M, Becker MW, Pihalja M, Weissman IL, et al. Bmi-1 is required for maintenance of adult self-renewing haematopoietic stem cells. Nature. 2003; 423:302–305. [PubMed: 12714971]

Schmitt CA, McCurrach ME, de Stanchina E, Wallace-Brodeur RR, Lowe SW. INK4a/ARF mutations accelerate lymphomagenesis and promote chemoresistance by disabling p53. Genes Dev. 1999; 13:2670–2677. [PubMed: 10541553]

Schmitt CA, Fridman JS, Yang M, Lee S, Baranov E, Hoffman RM, et al. A senescence program controlled by p53 and p16INK4a contributes to the outcome of cancer therapy. Cell. 2002; 109:335–346. [PubMed: 12015983]

Shimizu T, Ishikawa T, Sugihara E, Kuninaka S, Miyamoto T, Mabuchi Y, et al. c-MYC overexpression with loss of Ink4a/Arf transforms bone marrow stromal cells into osteosarcoma accompanied by loss of adipogenesis. Oncogene. 2010

Sugihara E, Kanai M, Saito S, Nitta T, Toyoshima H, Nakayama K, et al. Suppression of centrosome amplification after DNA damage depends on p27 accumulation. Cancer Res. 2006; 66:4020–4029. [PubMed: 16618721]

Tsuji K, Mizumoto K, Sudo H, Kouyama K, Ogata E, Matsuoka M. p53-independent apoptosis is induced by the p19ARF tumor suppressor. Biochem Biophys Res Commun. 2002; 295:621–629. [PubMed: 12099684]

Vassilev LT, Vu BT, Graves B, Carvajal D, Podlaski F, Filipovic Z, et al. In vivo activation of the p53 pathway by small-molecule antagonists of MDM2. Science. 2004; 303:844–848. [PubMed: 14704432]

Visvader JE. Cells of origin in cancer. Nature. 2011; 469:314–322. [PubMed: 21248838]

Wade M, Wang YV, Wahl GM. The p53 orchestra: Mdm2 and Mdmx set the tone. Trends Cell Biol. 2010; 20:299–309. [PubMed: 20172729]

Wang PY, Young F, Chen CY, Stevens BM, Neering SJ, Rossi RM, et al. The biologic properties of leukemias arising from BCR/ABL-mediated transformation vary as a function of developmental origin and activity of the p19ARF gene. Blood. 2008; 112:4184–4192. [PubMed: 18755985]

Wilson A, Murphy MJ, Oskarsson T, Kaloulis K, Bettess MD, Oser GM, et al. c-Myc controls the balance between hematopoietic stem cell self-renewal and differentiation. Genes Dev. 2004; 18:2747–2763. [PubMed: 15545632]

Yasuda T, Sanjo H, Pages G, Kawano Y, Karasuyama H, Pouyssegur J, et al. Erk kinases link pre-B cell receptor signaling to transcriptional events required for early B cell expansion. Immunity. 2008; 28:499–508. [PubMed: 18356083]
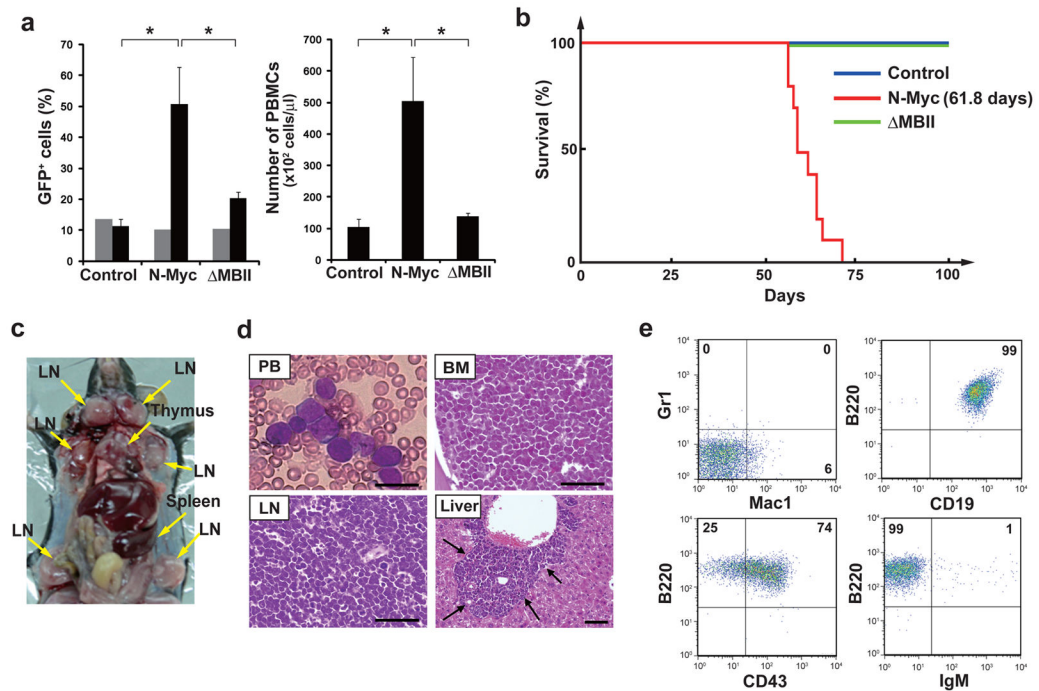
Figure 1. N-Myc expression in BM-MNCs induces pre-B ALL/LBL

(a), Left, percent of GFP$^+$ cells before transplantation in control, *N-Myc*- or ΔMBII-transduced BM-MNCs (gray) or 6 weeks after transplantation in PBMCs (solid) of mice. Right, number of PBMCs 6 weeks after transplantation in indicated mice. Data represent means ± SD. *, $P < 0.01$. (b), Survival curves of mice transplanted with empty-control (blue, n=10), *N-Myc* (red, n=10) or ΔMBII (green, n=8) -transduced BM-MNCs. (c), Representative tumor-bearing mouse transplanted with *N-Myc*-transduced BM cells showing enlarged LNs, thymus and splenomegaly. (d), Representative histopathology of peripheral blood (PB) stained with May-Giemsa, and bone marrow (BM), lymph node (LN) and liver stained with H&E in tumor-bearing mice. Arrows indicate invaded tumor cells. Scale bar = 20 μm in PB, 50 μm in tissues. (e), Flow cytometric immunophenotyping of GFP$^+$ BM cells from a tumor-bearing mouse transplanted with *N-Myc*-transduced BM-MNCs.
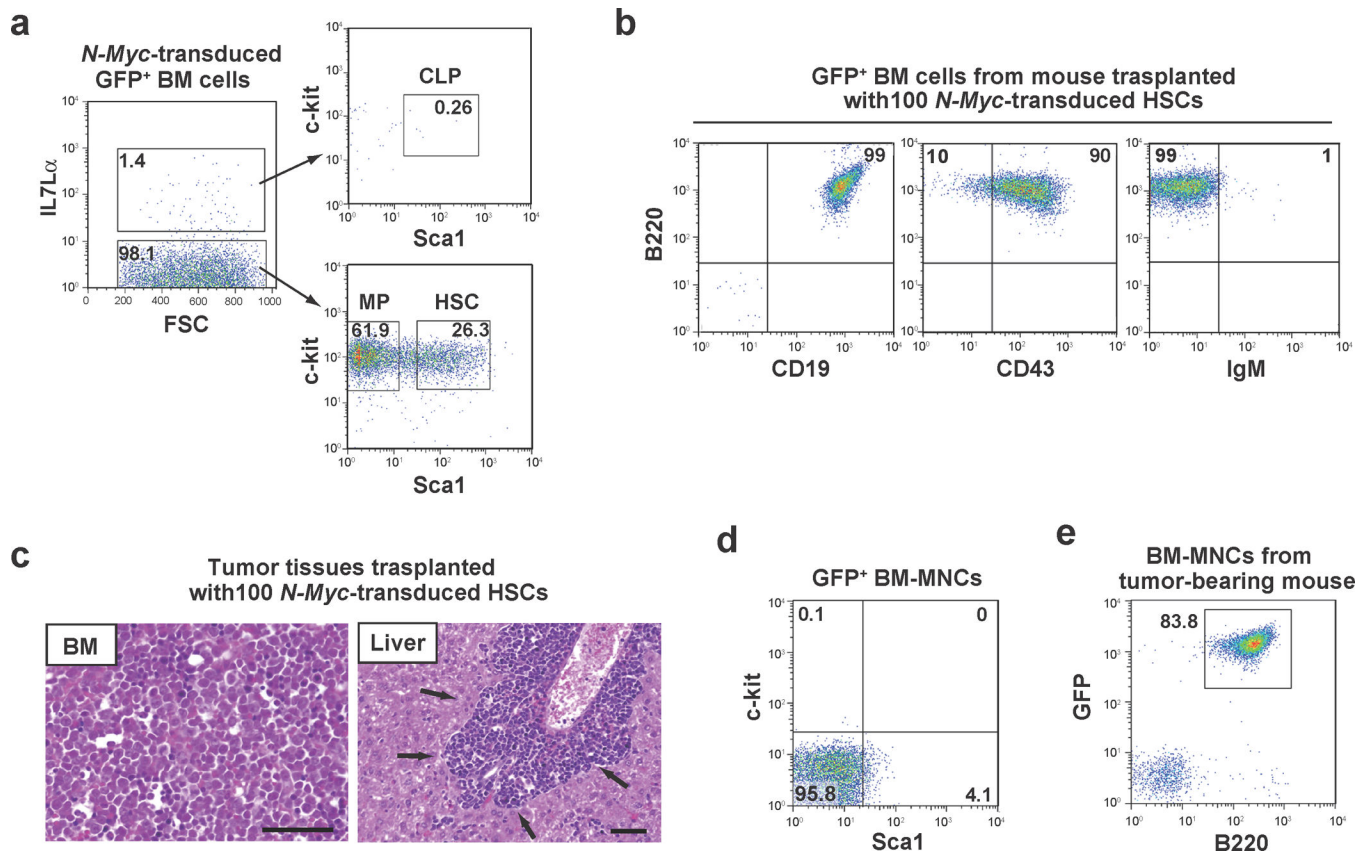
Figure 2. HSCs are highly susceptible to N-Myc-induced Pre-B ALL/LBL
(a), GFP+ *N-Myc*-transduced BM-MNCs were fractionated into Lin− IL7Rα−c-Kit+ Sca1+ cells (HSCs) or Sca1− cells (MPs), or IL7Rα+ c-Kit+ Sca1+ cells (CLPs). (b), Flow cytometric immunophenotyping of GFP+ BM cells from a mouse transplanted with 100 *N-Myc*-transduced HSCs. (c), Representative histopathology of BM and liver stained with H&E from a mouse transplanted with *N-Myc*-transduced HSCs. Arrows indicate invaded tumor cells. Scale bar = 50 μm. (d), Representative flow cytometric plot of Sca1 and c-kit expression in GFP+ BM-MNCs derived from mice transplanted with *N-Myc*-transduced HSCs. (e), Representative flow cytometric plot of the GFP+ B220+ cell subpopulation of BM-MNCs derived from mice transplanted with *N-Myc*-transduced HSCs.
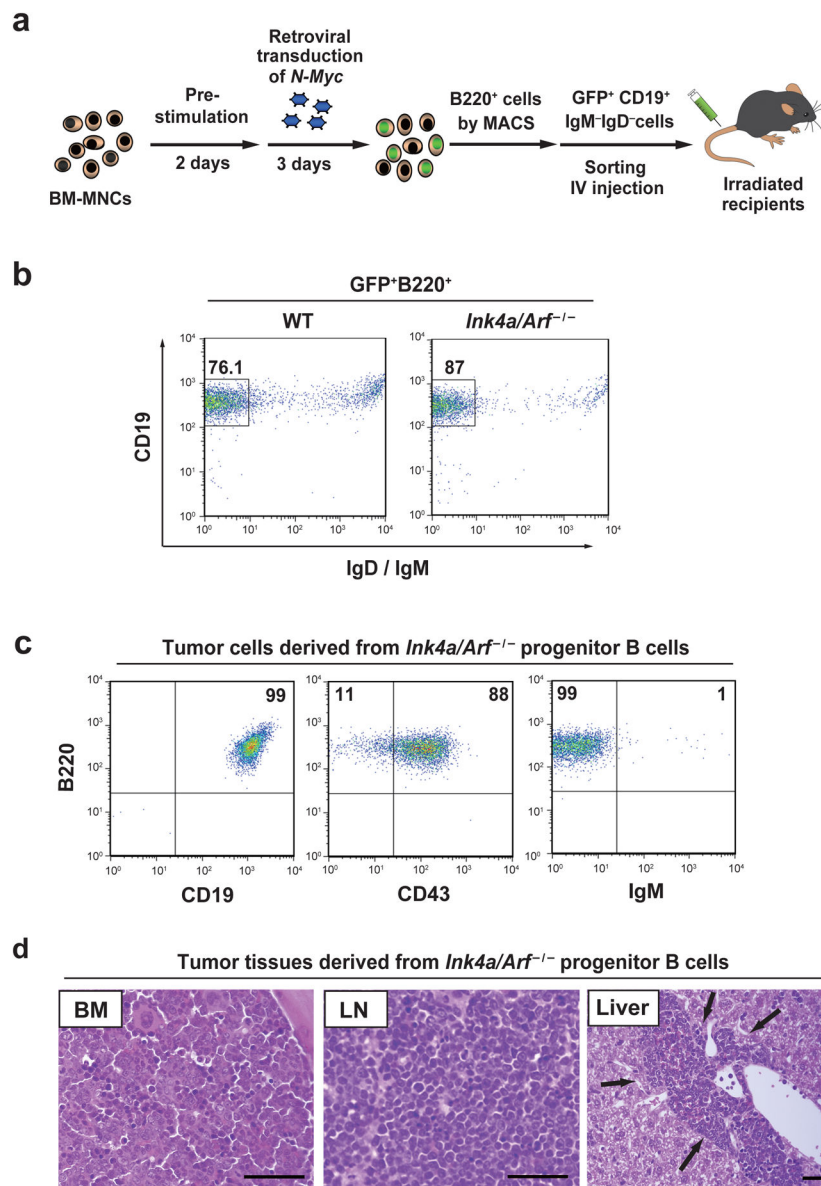
Figure 3. N-Myc directly induces pre-B ALL/LBL from committed B cell progenitors from *Ink4a/Arf*−/− mice

(a), Experimental design for the isolation of progenitor B cells (GFP+ B220+ CD19+ IgM− IgD−) from *N-Myc*-transduced BM cells. (b), Representative flow cytometric plots of the progenitor B cell subpopulation of *N-Myc*-transduced BM cells from WT or *Ink4a/Arf*−/− mice. (c) Flow cytometric immunophenotyping of GFP+ BM cells from a mouse transplanted with *Ink4a/Arf*−/− progenitor B cells. (d), Representative histopathology of BM and liver stained with H&E from mice transplanted with *Ink4a/Arf*−/− progenitor B cells. Arrows indicate invaded tumor cells. Scale bar = 50μm.
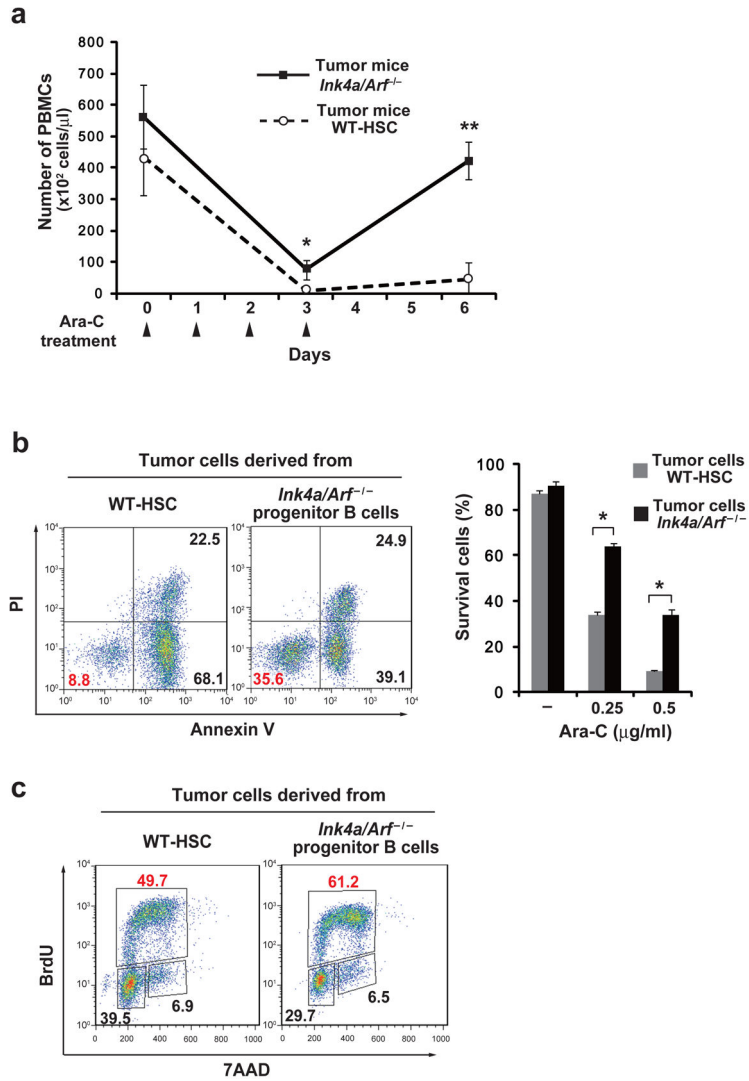
Figure 4. Tumor cells derived from _Ink4a/Arf_$^{-/-}$ progenitor B cells are more resistant to Ara-C treatment than those from WT-HSCs _in vitro_ and _in vivo_.
(a), Four doses of daily Ara-C (100 mg/kg) were administered i.p. to tumor-bearing mice transplanted with _N-Myc_-transduced WT HSCs or _Ink4a/Arf_$^{-/-}$ progenitor B cells. Following Ara-C injection on day 0, the number of PBMCs in each mouse was monitored every three days. Arrowheads indicate the schedule of Ara-C dosing. Data represent means ± SD; n = 3. *, $P < 0.05$, **, $P < 0.01$. (b), Primary cultured tumor cells derived from WT HSCs or _Ink4a/Arf_$^{-/-}$ progenitor B cells were treated with Ara-C for 48 h and subjected to Annexin V assay. Representative plots are shown in the left panels. Percent of Annexin V-negative cells is shown in the graph on the right. Data represent means of triplicates ± SD. *, $P < 0.01$. (c), BrdU incorporation cell cycle analysis of tumor cells derived from WT HSCs or _Ink4a/Arf_$^{-/-}$ progenitor B cells. Numbers for each gate (lower left, upper and lower right) indicate percent of cells in G1 phase, S phase and G2-M phase, respectively. Plots are representative of two independent experiments.
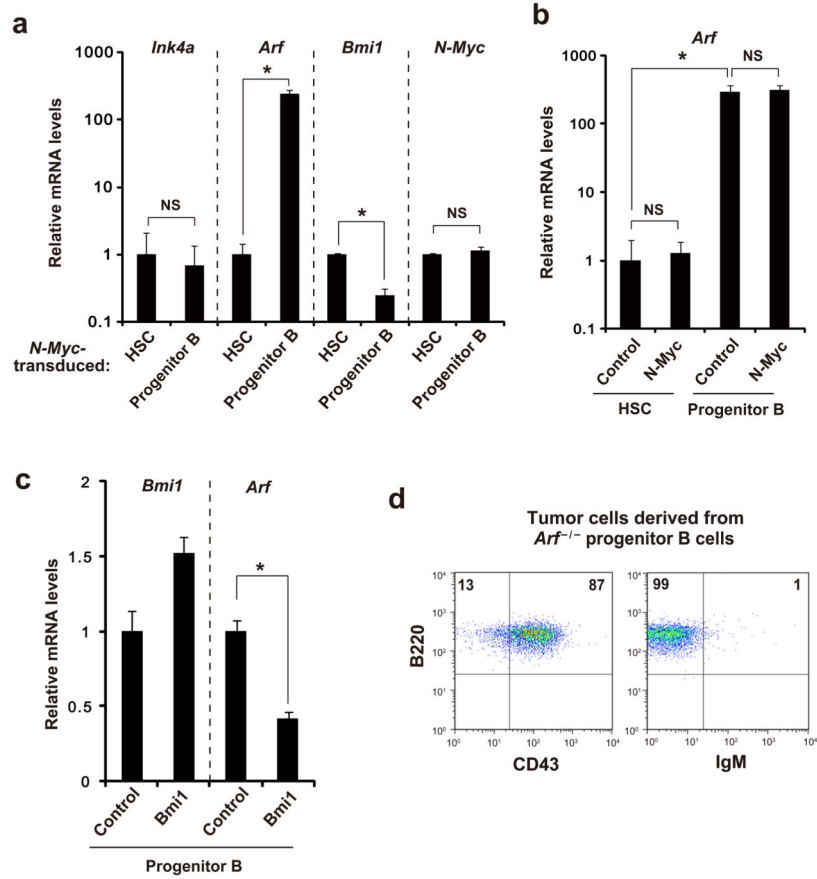
Figure 5. *Arf* has a key role in blocking pre-B ALL/LBL induced by N-Myc in progenitor B cells
(a), mRNA expression of *Ink4a, Arf*, *Bmi1* and *N-Myc* as determined by quantitative real-time RT-PCR in *N-Myc*-transduced HSCs and progenitor B cells. (b), mRNA expression of *Arf* in control- or *N-Myc*-transduced HSCs and progenitor B cells. (c), mRNA expression of *Bmi1* and *Arf* in control- or *Bmi1*-transduced progenitor B cells. (d), Flow cytometric immunophenotyping of tumor cells from a mouse transplanted with *N-Myc*-transduced *Arf*^{−/−} progenitor B cells. Data in (a), (b) and (c) represent means of triplicates ± SD. *, $P < 0.05$. NS: not significant.
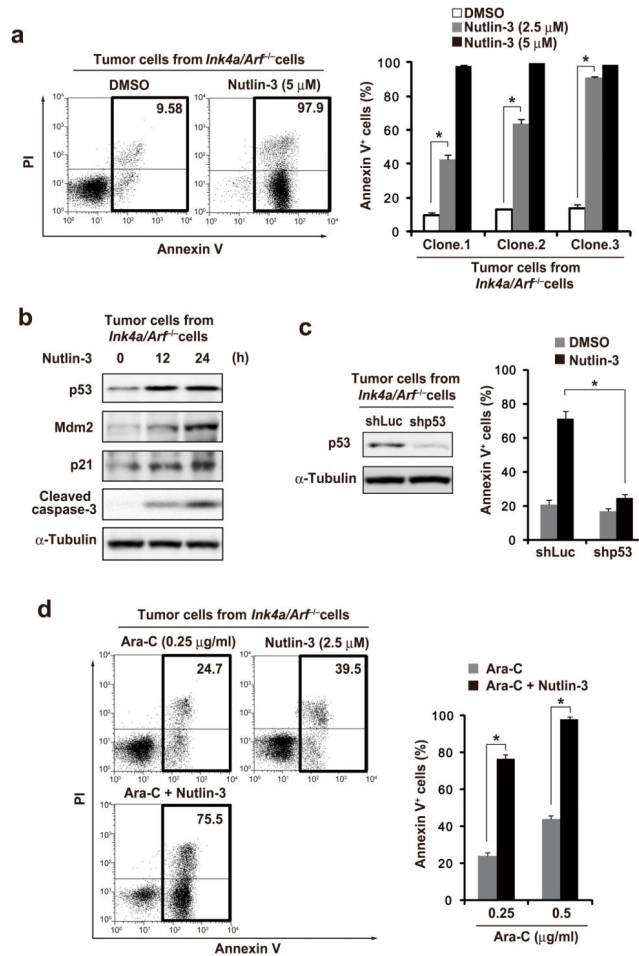
Figure 6. The Mdm2 inhibitor Nutlin-3 effectively kills tumor cells derived from *Ink4a/Arf*$^{-/-}$ progenitor B cells

(a), Left, results of an Annexin V assay of tumor cells (clone 1) derived from an *Ink4a/Arf*$^{-/-}$ progenitor B cells following treatment with Nutlin-3 or DMSO for 48 h. The numbers shown in each panel indicate the percentage of Annexin V-positive cells. Right, tumor cells (clones 1, 2 and 3) derived from an *Ink4a/Arf*$^{-/-}$ progenitor B cells were treated with Nutlin-3 or DMSO for 48 h. Percentage of Annexin V-positive cells after Nutlin-3 treatment is shown. (b), Immunoblot analysis of the expression of p53, Mdm2, p21 and cleaved caspase-3 in tumor cells (clone 1) from an *Ink4a/Arf*$^{-/-}$ progenitor B cells 0, 12 and 24 h after Nutlin-3 (2.5 μM) treatment. α-Tubulin was analyzed as a loading control. (c), Left, immunoblot analysis of the expression of p53 in *Ink4a/Arf*$^{-/-}$ derived tumor cells expressing *p53* shRNA (shp53) or *luciferase* shRNA(shLuc). Right, percentage of Annexin V-positive cells 48 h after Nutlin-3 (2.5μM) or DMSO treatment in *Ink4a/Arf*$^{-/-}$ derived tumor cells expressing *p53* shRNA or *luciferase* shRNA. (d), Left, results of an Annexin V assay of cultured tumor cells (clone 1) from an *Ink4a/Arf*$^{-/-}$ progenitor B cells 48 h after treatment with Ara-C (+ DMSO), Nutlin-3, or a combination of Ara-C and Nutlin-3. Right, percentage of Annexin V-positive cells 48 h after combination treatment with Ara-C and Nutlin-3 (2.5μM) is shown. Data in (a), (c) and (d) represent means of triplicates ± SD. *, $P < 0.01$.
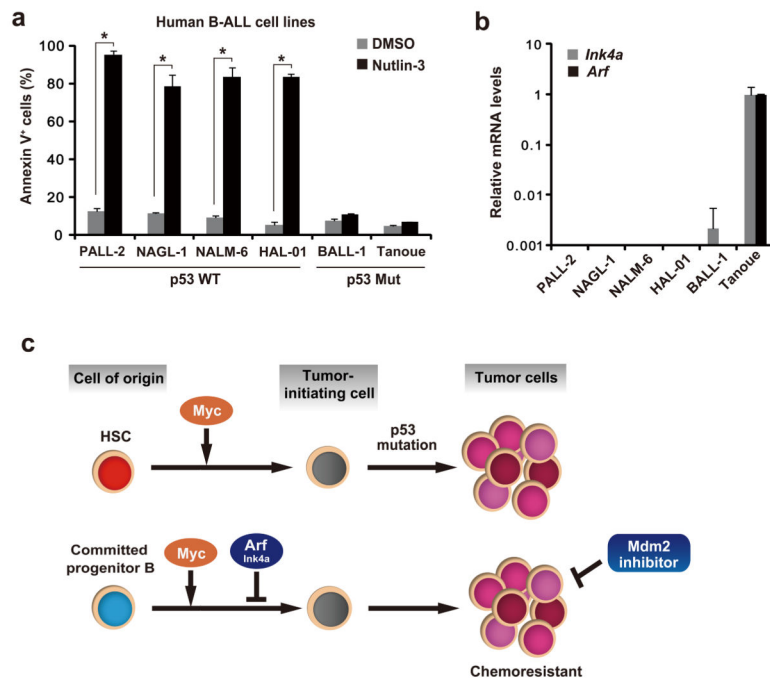
Figure 7. Human B-ALL cell lines with wild type p53 lack Ink4a and Arf expression and are sensitive to Nutlin-3

(a), percentage of Annexin V-positive cells 48 h after Nutlin-3 (5 μM) or DMSO treatment in human B-ALL cell lines. p53 WT and p53 Mut indicate the cell lines with wild type p53 and mutated p53, respectively. Data represent means of triplicates ± SD. *, $P < 0.01$. (b), mRNA expression of *Ink4a, Arf* as determined by quantitative real-time RT-PCR in human B-ALL cell lines. Data represent means of triplicates ± SD. (c), Schematic model of the mechanisms by which Myc induces pre-B ALL/LBL from the different cells of origin.

Table 1

Summary of transplantation analysis using *N-Myc*-transduced hematopoietic stem cells, CLPs and MPs.

Transplanted cell population	Transplanted cells (#)	Transplanted mice (#)	Tumor mice	Latency (days)	Frequency of tumor-initiating cells	P
HSCs	10000	4	4	61.5		
	1000	5	5	77.5	1:184	-
	100	5	2	91		
CLPs	1000	2	2	75.5		
	100	4	0	-	1:558	0.261
MPs	10000	4	3	81		
	1000	5	0	-	1:9286	< 0.01
	100	5	0	-		

Table 2

Summary of secondary transplantation analysis using GFP[+] B220^{+} cells from BM-MNCs derived from tumor-bearing mice transplanted with *N-Myc*-transduced HSCs

Transplanted cell population	Transplanted cells (#)	Transplanted mice (#)	Mice with tumor (#)	Latency (days)	Frequency of tumor-initiating cells
GFP[+] B220[+] BM-MNCs	5000	6	6	32.1	
	1000	6	6	44.3	1:216
	100	6	2	49.8	

Table 3

Summary of transplantation analysis using *N-Myc*-transduced progenitor B cells from WT or *Ink4a/Arf*^{-/-} mice

Transplanted cell population	Transplanted cells (#)	Transplanted mice (#)	Mice with tumor (#)	Latency (days)	Frequency of tumor initiating cells
Progenitor B cells from WT mice	50000	2	0	-	-
	10000	4	0	-	
Progenitor B cells from *Ink4a/Arf*^{-/-} mice	50000	2	2	35.5	
	10000	4	4	51.6	1:2109
	1000	3	1	61	